Digest Journal of Nanomaterials and Biostructures Vol. 7, No. 4, October-December 2012, p. 1709-1717

# MORPHOLOGICAL AND STRUCTURAL ASPECTS OF SOME FERROSPINEL NANOPOWDERS FOR CATALYST APPLICATIONS

N. REZLESCU[a*], E. REZLESCU[a], P.D. POPA[a], E. POPOVICI[b], C. DOROFTEI[a,c], M. IGNAT[a,b], A.C. BARBINTA[d]
[a]*National Institute of Research and Development for Technical Physics, Iasi, Romania*
[b]*Al. I. Cuza University, Chemical Faculty. Iasi, Romania*
[c]*Al. I. Cuza University, Physics Faculty, Iasi, Romania*
[d]*Gh. Asachi Technical University, Faculty of Mechanics, Iasi, Romania*

The $Me_xFe_{3-x}O_4$ (x = 1 for divalent metal, Me = Mg, Co, Ca and x = 0.5 for monovalent metal Me = Li) ferrites were prepared by self-combustion method and then heat treated at $900^0$C to assure chemical and thermal stability for catalyst applications. The morphological and structural characterization of the ferrite powders have been performed with various techniques: X-ray diffraction (XRD) to determine the phase composition and the crystallite nanosize, SEM observations to show off the agglomerate formations, EDAX spectroscopy to evaluate the chemical composition and BET analysis to determine the specific surface area. The ferrite powders have been tested as catalysts in combustion reaction of three diluted gases: acetone/air, ethanol/air and methanol/air. The results revealed a dependence of the gas combustion minimum temperature on the ferrite catalyst composition. The gas combustion process over Mg ferrite surface can start at lower temperatures than over the other ferrites.

(Received September 11, 2012; Accepted October 30, 2012)

*Keywords:* Metal oxides (ferrites), Selfcombustion, microstructure, XRD and EDAX, scanning electron microscopy (SEM), catalyst, nanopowder

## 1. Introduction

In the last years there is an interest in investigating the catalytic combustion of hydrocarbons using ferrospinel-type metal oxide compounds as catalysts. The catalytic combustion makes possible to drastically reduce the temperature required for a complete combustion. Thus, while thermal combustion proceeds at temperatures above $1000^o$C, in the catalytic process the temperature for a complete combustion can be below $700^0$C.

The main objective is to find a thermally and chemically stable solid-state catalyst to ignite the combustible gases at low temperature, without the use of flames. Current catalyst compositions that have shown promising results are based on transition metal oxide compounds.

Several research reports [1 - 6] have proven that the spinel ferrites (ferrospinels) have a great potential not only as a refractory material, but also as a catalytic material for the combustion of the volatile organic compounds (VOC), given their high melting point, hardness, thermal and chemical stability and low cost.

For catalytic purposes, the microstructure has a predominant role. The achievement of ferrites with the high specific surface areas and nanosized particles is a priority in the performance of a ferrite catalyst. In nanostructured ferrites, the interface between the nanoparticles and its surrounding media plays a major role compared to the bulk. Also, the strong curvature of ferrite particles due to their small radius leads to an increased number of the structural defects at the

*Corresponding author: reznic@phys-iasi.ro; nicolae.rezlescu@gmail.com

nanoparticle surface which enhance the surface reactivity. To obtain spinel ferrites with superior microstructures, various chemistry based synthesis methods have been proposed, such as sol-gel technique [7], coprecipitation [8, 9], citrate precursor [10, 11], hydrothermal synthesis [12, 13], spray drying [1], combustion reaction [1], and flash combustion method [14]. In this work, self-combustion method [15 – 17] was applied to synthesize ferrite nanoparticles. Among the various methods known, the self-combustion method allows a good control over the size of the material particles, which in turn decides their structural properties. The procedure offers the advantage to produce ultra-fine, homogeneous and reproducible, multicomponent ceramic powders and with precise stoichiometry. The preparation way is relatively simple, implies a low energy cost by utilizing an exothermal reaction and allows a controlled growth of the crystallites by subsequent heat treatments.

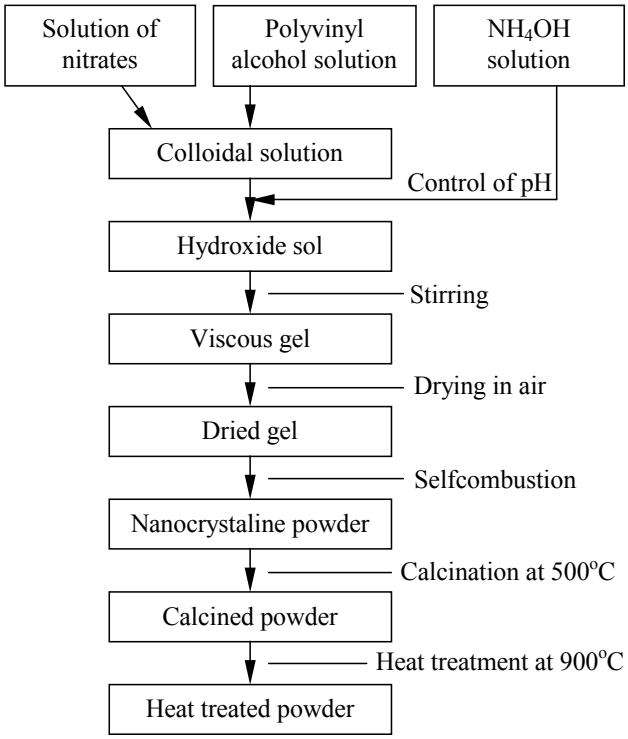


*Fig.1 Processing of ferrite powders by self-combustion route.*

The purpose of this work was to find new ferrite compositions with suitable properties for catalyst applications. Spinel-type ferrite nanopowders of chemical composition $Me_xFe_{3-x}O_4$ (x = 1 for divalent metal, Me = Mg, Co, Ca and x = 0.5 for monovalent metal Me = Li) were prepared through self-combustion procedure. Some structural and morphological aspects of the four ferrite nanopowders were investigated to clarify how compositional changes affect properties and characteristics of ferrites.

X-ray diffraction (XRD), nitrogen adsorption by BET, scanning electron microscopy (SEM) and energy dispersive X-ray (EDAX) techniques were used to investigate the structural and chemical properties. The catalyst activity of the ferrite powders was tested. It is known that the starting temperature for combustion reaction of volatile organic compounds (VOC) depends on the composition of the catalyst and the nature of the compound to be oxidized [18]. The minimum temperature of the catalytic combustion reaction of diluted gases (ethanol/air, methanol/air and acetone/air) over ferrite nanopowder catalysts was determined and the effect of Me-type was analyzed.

The catalytic combustion has received much attention mainly due to the possibility of lowering the combustion temperature thus practically reducing emissions of $NO_x$, CO and unburned hydrocarbons [19].

## 2. Experimental

The synthesis of $MgFe_2O_4$, $CaFe_2O_4$, $CoFe_2O_4$ and $Li_{0.5}Fe_{2.5}O_4$ spinel ferrite particles was accomplished through self-combustion route. In this method, the thermal energy for synthesis reaction of ferrites was provided by a quick exothermic reaction. Metal nitrates, ammonium hydroxide and polyvinyl alcohol were used as starting materials. Metal nitrates are the salts we preferred because they contain nitrogen and are water soluble (a good homogenization can be achieved in solution). Hydrate salts are even more favored, although the water molecules are irrelevant for the chemistry of the combustion. The preparation procedure by self-combustion is given in Fig.1. This route included the following procedures: (1) dissolution of metal nitrates in deionized water; (2) polyvinyl alcohol addition to the first solution to make a colloidal solution; (3) $NH_4OH$ addition to increase pH to about 8; (4) stirring at $80^0$C; (5) drying the gel at $120^0$C; (6) and finally self-combustion. The dried gel was ignited at one end by using an electrically heated W wire (0.5 mm in diameter) and an exothermic combustion reaction began. The combustion front spontaneously autopropagates and converts the dried gel in a loose powder. The as burnt powders were calcined at $500^o$C for 30 min to eliminate any residual organic compounds. Then, calcined powders were heat treated at $900^0$C for a short time of 10 minutes, to obtain a good crystallinity of the powder without a sesizable increase of the crystallites. The detailed step-by-step procedure has been reported elsewhere [15 - 17].

The structural homogeneity, crystal structure, phase formation and crystallite size were determined by X-ray diffraction (XRD), using PANANALYTICAL X' PERT PRO MPD diffractometer and CuKα radiation (λ = 1,542512 Å). The diffraction patterns were recorded in the range $2\theta = 20 \div 80^0$ at $2^0 min^{-1}$. The average crystallite size was calculated from Scherer's equation [20]

$$D_{XRD} = 0.9\lambda / \beta \cos\theta, \quad (1)$$

where λ is the wavelength of the target, β is the full width maximum of diffracted (311) plane and θ is Bragg angle.

The surface morphology was examined with scanning electron microscope (QUANTA 2000 3D Dual beam model). The specific surface area ($S_{BET}$) was calculated from the nitrogen sorption data using the Brunauer-Emmett-Teller (BET) equation [21]. Adsorption/desorption isotherms of nitrogen were measured at ~ 77K with NOVA 2200 apparatus. The pore size distribution (PSD) curves were obtained from the sorption isotherms using BJH (Barret, Joyner and Halenda) method [21]. The chemical composition of the ferrite particles was determined with an energy dispersive X-ray spectrometer (EDAX: Genesis). Incident electron beam energies from 0 to 14 Kev have been used. In all cases the beam was at normal incidence to the sample surface and the measurement time was 100 s. All the EDAX spectra were corrected using the ZAF correction.

## 3. Results and discussions

The X-ray powder diffraction was employed for phase identification and nanoparticle formation. The XRD patterns of the ferrite powders before and after heat treatment at $900^0$C are shown in Fig.2. Except for Ca-containing composition, the cubic spinel phase formation with Fd3m space group for Co, Mg and Li ferrites was detected before and after heat treatment at $900^0$C. The most intense peaks in all specimens are (220), (311), (400), (422), (333) and (440). Monophase crystalline materials were obtained.

After calcination at $500^0$C for 30 min dicalcium ferrite, $Ca_2Fe_2O_5$ (Fig.2 - a) was formed, with orthorhombic brownmillerite structure belonging to the space group Pcmn with lattice parameters: a = 5.42 Å, b = 14.77 Å and c = 5.59 Å. $Ca_2Fe_2O_5$ brownmillerite structure regarded as

an oxygen-deficient perovskite ($ABO_{2.5}$) provides oxidation catalytic activity and makes this ferrite a good candidate as a toxic-metal free and a low-cost catalyst [2]. By heat treatment at $900^0$C for 10 min, $CaFe_2O_4$ phase with orthorhombic structure (space group Pnam) was detected (Fig.2 - b). The lattice parameters are given in Table 1.

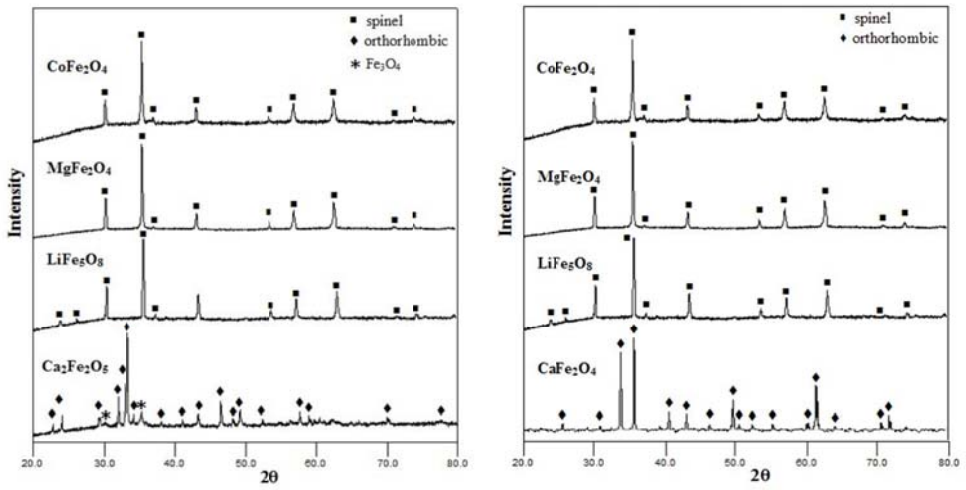


( a ) ( b )

*Fig.2 XRD patterns for the ferrite powders: (a) after calcination at $500^0$C; (b) after heat treatment at $900^0$C*

*Table 1 Structure characteristics of ferrites after $900^0$C heat treatment*

| Ferrite composition | Metal ion radius (nm) | Lattice constant (nm) | Crystallite size (nm) | X-ray density ($g/cm^3$) |
|---|---|---|---|---|
| $CoFe_2O_4$ | 0.079 | 0.8379 (0.838) | 36.33 | 5.31 |
| $MgFe_2O_4$ | 0.086 | 0.8366 (0.836) | 41.78 | 4.55 |
| $LiFe_5O_8$ | 0.090 | 0.8338 (0.833) | 46.44 | 4.74 |
| $CaFe_2O_4$ | 0.114 | a = 0.9230 b = 1.070 c = 0.3029 | 51.93 | 4.79 |

The results obtained by XRD analysis are summarized in Table 1 for ferrite powders after heat treatment at $900^0$C. Some observations can be made:

- the lattice constant depends on the Me type and suggests the formation of a compositionally homogeneous solid solution;
- the lattice constants for ferrite nanoparticles are close to those known for bulk ferrites [22] (are given in parenthesis);
- the crystallite size $D_{XRD}$ calculated with Scherer's equation was found to be in the range 36 to 52 nm and this demonstrates that powders with nanosized crystallites have been obtained;
- though all samples were prepared under identical conditions, the crystallite size was not the same for all compositions; this increases with increasing the Me ion radius [23].

The X-ray density, $d_X$, was calculated with the formula [22]

$$d_X = 8M / Na^3 \quad , \tag{2}$$

where M is molecular mass, N is Avogadro number and a is lattice constant.

Nitrogen adsorption/desorption at ~ 77 K was used to obtain the informations about the specific surface area $S_{BET}$ and the pore volume of the ferrite particles. Some characteristic isotherms are presented in Fig. 3 for samples before and after heat treatment at $900^0$C. These isotherms can be classified as type II in IUPAC classification [21]. The pore size distribution graphs (PSD) obtained from $N_2$ sorption isotherms by BJH method [21] are shown inset of Fig.3.

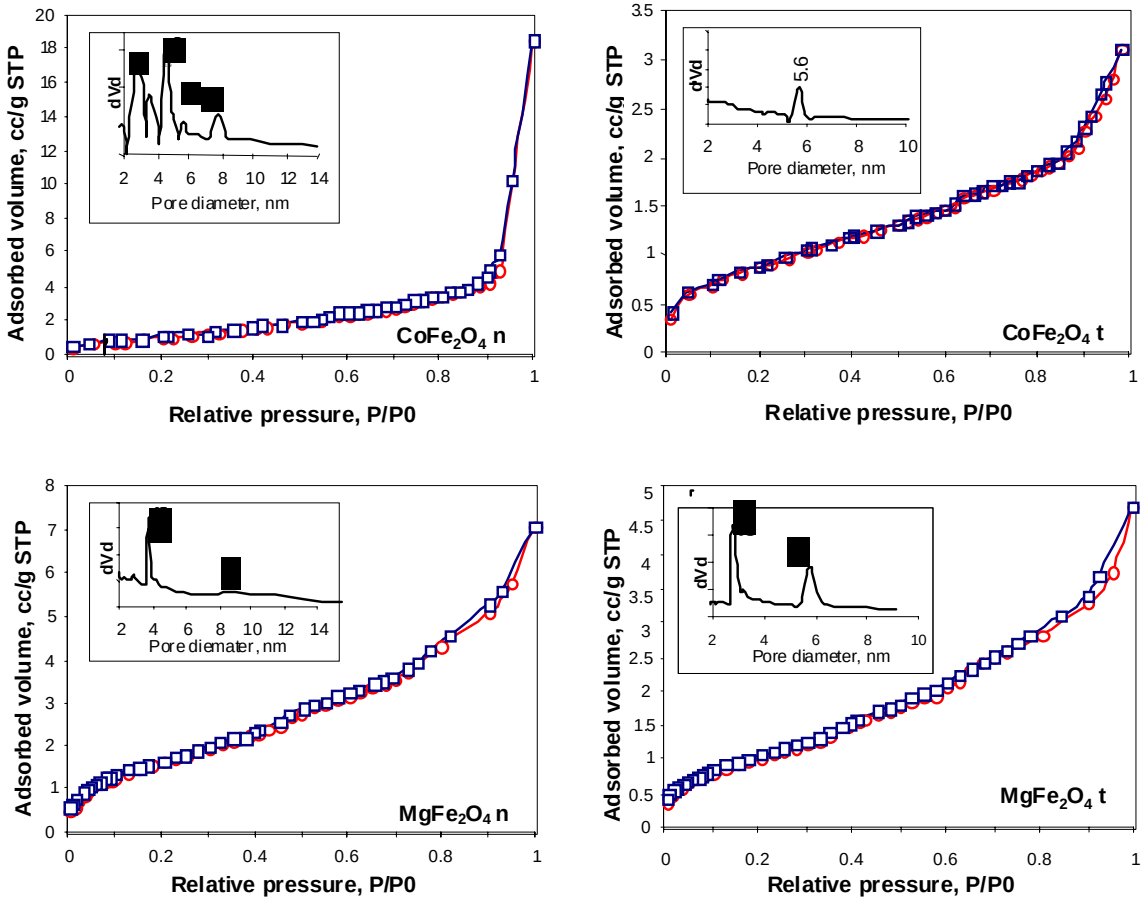


*Fig. 3 Nitrogen adsorption/desorption isoterms at 77K for two ferrite powders (◦◦◦ is the adsorption branch and ▫▫▫ is the desorption branch; n – samples after calcination at $500^0$C and t – samples after heat treatment at $900^0$C; inset: the pore size distribution graphs)*

The obtained results for all samples heat treated at $900^0$C for 10 min are summarized in Table 2. $D_{BET}$, was calculated using the $S_{BET}$ measured values (by assuming that all particles have spherical shape) with the formula [21]

$$D_{BET} = 6/S_{BET} d_X , \qquad (3)$$

where 6 is the shape factor and $d_X$ is the X-ray density. One can see from Table 2 that the surface areas, $S_{BET}$, have reasonable values, in the range 3.91 – 2.77 $m^2$/g and the particle diameter ranges between 337 and 455 nm. The pore volume is very small (0.06 – 0.038 cc/g). The pore volume and particle size markedly influence the surface area. It is interesting to note that the Mg ferrite has the largest $S_{BET}$ and pore volume, yet these are smaller than those measured on the samples calcined at $500^0$C, but without heat treatment at $900^0$C. For comparison, in Table 3 are given $S_{BET}$, $D_{BET}$ and pore volume for Mg- and Co- ferrites calcined at $500^0$C. One can see that the particle diameter increased after annealing at $900^0$C. This increase is probably due to the presence of nanometric particles which favor the coalescence. Although $S_{BET}$ value of the thermal treated samples is smaller, these samples were chosen for investigation because the annealing at $900^0$C assures the good thermal and chemical stability required by catalyst applications.

*Table 2 Surface characteristics for ferrites after $900^0C$ heat treatment*

| Ferrite composition | $S_{BET}$ ($m^2/g$) | $D_{BET}$ (nm) | Pore volume (cc/g) | Adsorbed $N_2$ volume (cc/g) |
|---|---|---|---|---|
| $CoFe_2O_4$ | 3.26 | 346 | 0.0048 | 3.2 |
| $MgFe_2O_4$ | 3.91 | 337 | 0.006 | 4.8 |
| $LiFe_5O_8$ | 2.77 | 455 | 0.0038 | 2.5 |
| $CaFe_2O_4$ | 2.83 | 441 | 0.0049 | 3.3 |

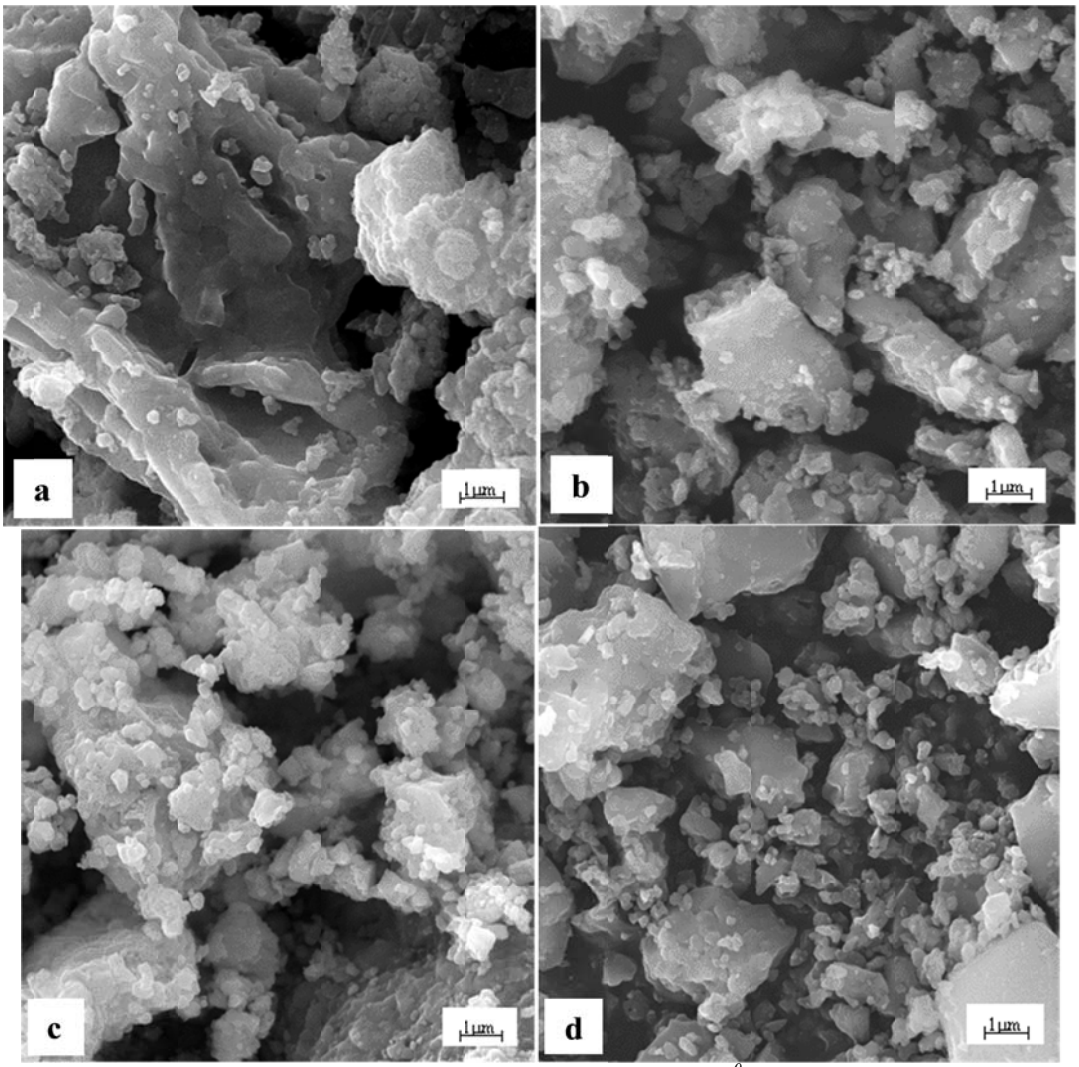


*Fig.4 SEM micrographs for ferrites after heat treatment at $900^0C$: a) $MgFe_2O_4$; b) $LiFe_5O_8$; c) $CoFe_2O_4$; d) $CaFe_2O_4$.*

*Table 3 Surface characteristics for two ferrites calcined at $500^0C$*

| $S_{BET}$ ($m^2/g$) | $D_{BET}$ (nm) | Pore volume (cc/g) |
|---|---|---|
| 3.61 | 313 | 0.0287 |
| 6.35 | 207 | 0.090 |

From PSD spectra, shown inset of Figure 3, one can see that the pore sizes are in the mesoporous range (5÷15 nm) and the pore distribution changes with the Me-type and the thermal treatment. The pore volume is correlated with adsorbed $N_2$ volume.

The surface morphology of ferrite powders heat treated at $900^0$C was examined by SEM and it is illustrated in Fig. 4. It is clear from the micrographs that the microstructure changes with changing the Me-type in the ferrite composition. One can notice the presence of both mini- and macro-agglomerates of irregular shapes. The particles within the agglomerations are small (340 – 450 nm). The Ca and Li ferrites exhibit only some large agglomerates and many dispersed small agglomerates (about of 1 μm) due to the coarse particles (of about 450 nm). In Co and Mg ferrites, the finer granulation of the powders (of about 340 nm) led to the formation of many large agglomerates (4÷5 μm). All agglomerates are soft and can be easily destroyed by light grinding.

The EDAX patterns confirm the homogeneous mixing of Mg, Li, Ca, Co and Fe atoms in samples and the purity of the chemical compositions. The Me/Fe molar ratio was found close to the theoretical value. EDAX spectrum for $MgFe_2O_4$ powder is shown in Fig. 5. One can see characteristic peaks and the composition of $MgFe_2O_4$ ferrite. The Mg/Fe molar ratio was found of 0.55, whereas theoretical value is of 0.5 which is a proof of homogeneous distribution of the elements in the solid.

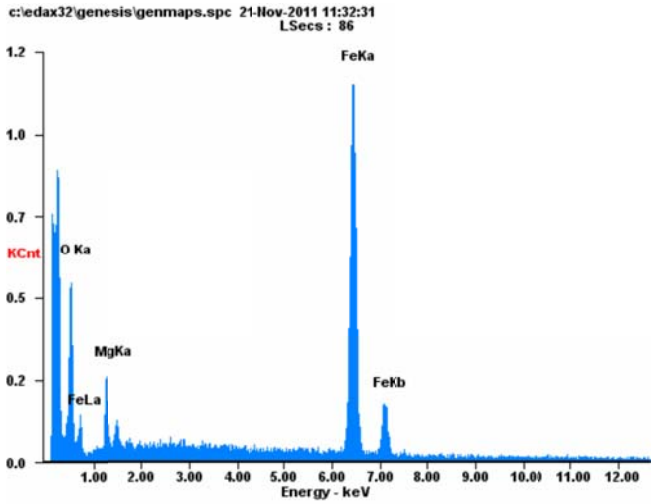


| Element | Wt% | At% |
|---|---|---|
| **OK** | 26.66 | 50.34 |
| **MgK** | 14.21 | 17.66 |
| **FeK** | 59.13 | 31.99 |

*Fig.5. EDAX spectrum for $MgFe_2O_4$ ferrite heat treated at $900^0$C.*

The catalyst tests of the four prepared ferrite powders were performed by measuring the minimum temperature at which the combustion reaction of very small concentrations of acetone, ethanol and methanol occurs in air environment catalyzed by ferrite powders. It is known that the catalyzed combustion reaction takes place at much lower temperatures than that non-catalyzed. In Fig.6 the minimum temperature for combustion of the three diluted gases over the four ferrite nanopowders are given. For comparison is given also the minimum temperature required to ignite the mentioned gases without a spark or catalyst being present. All experiments were conducted twice to ensure reproducibility; similar results were always obtained. In the bar diagram one can remark the change of minimum combustion temperature with ferrite catalyst composition. It is important to note that the most efficient ferrite catalyst is Mg-ferrite which has the greatest effect in decreasing the combustion temperature (to about 200 deg) of gases in air environment, being the most active catalyst.

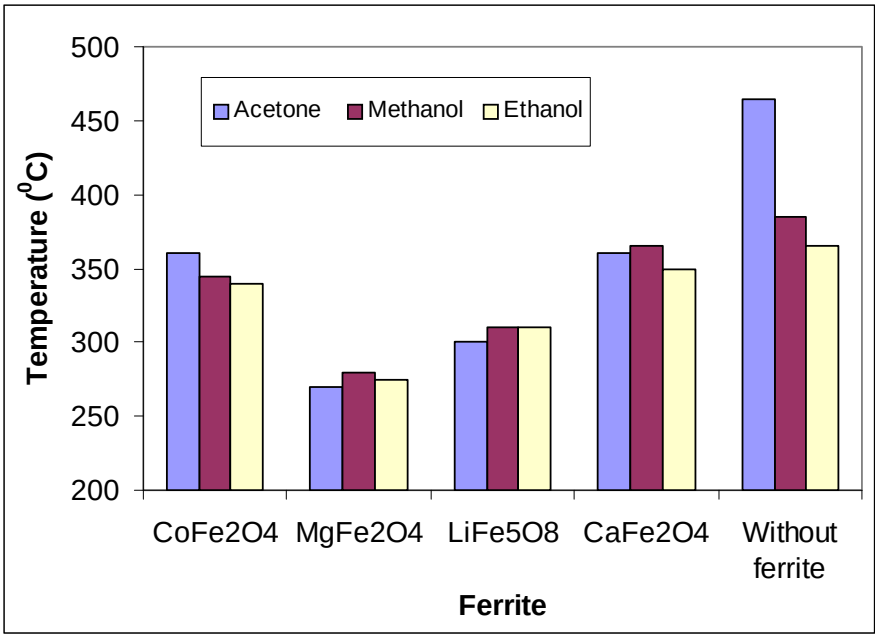


*Fig.6 Bar diagram for the minimum combustion temperature of acetone, ethanol and methanol vapour in air in the presence of ferrite catalyst and without catalyst*

It is known that the oxygen species ($O^{2-}, O_2^-, O^-$) adsorbed on the oxide compound surface play a major role in the catalytic combustion [24 - 26]. The interaction of surface active oxygen species with reactants determines the mechanism for gas oxidation over mixed oxide catalysts, but the surface defects are sites for oxygen adsorption [27]. However, the possibility of involvement of the surface lattice oxygen in the gas combustion over mixed oxides cannot be excluded [21]. The valence of $Mg^{2+}$, $Li^+$, $Ca^{2+}$ or $Co^{2+}$ ions, lower than that of $Fe^{3+}$ ion, can cause the formation of oxygen vacancies and modification of the lattice oxygen mobility.

In the present study, a possible explanation for the temperature differences in the gas combustion reactions catalyzed by various composition ferrites can be either different reactivity of the oxygen species adsorbed on the ferrite surfaces ($O^-$ is more active than $O^{2-}$) or various densities of the active surface sites. The improved activity of Mg containing ferrite can be mainly ascribed to a larger density of surface active oxygen species, weakly bonded on the ferrite surface, which can facilitate the ferrite to oxidize the combustible gas when this comes into contact with ferrite surface. Also, the larger surface area of Mg ferrite presumes much more intensive interactions between the ferrite surface and the gas which can promote the gas oxidation at lower temperatures. The weakly effect of Ca and Co ferrites suggests less active oxygen species available for the combustion reaction.

The obtained results incite to investigate also other ferrite compositions to find a catalytic material with the best properties.

## 4. Conclusions

The synthesis by nonconventional method, self-combustion, has favored the production of Mg-, Li-, Co- and Ca ferrite powders with nanometric crystallites.

The X-ray diffraction confirmed the crystallinity and the nanosize of the ferrite crystallites (36 – 52 nm).

SEM micrographs evidenced the presence of agglomerates of fine particles. The agglomerate sizes are in the range from 1 to 5 μm.

The specific surface area $S_{BET}$ and the pore volume obtained from nitrogen adsorption/desorption isotherms depend on the ferrite composition; Mg ferrite has the largest $S_{BET}$ and pore volume.

The catalytic tests revealed that the minimum temperature for catalytic combustion of diluted gases in air environment remarkably decreases when using Mg ferrite powder as catalytic material. A probable explanation has been proposed.

**Acknowledgements**

This work was supported by a grant of the Romanian National Authority for Scientific Research, CNST – UEFISCDI, project number PN-II-ID-PCE-2011-3-0453.

## References

[1] A.C.F.M. Costa, R.T. Lula, R.H.G.A.Kiminami, L.F.V. Gama, A.A. de Jesus, H.M.C. Andrade, J. Mater. Sci. **41**, 4871 (2006).
[2] Daisuke Hirabayashi, TakeshiYosikawa, Yoshiki Kawamoto, Kazuhiro Mockizuki, Kenzi Sukuki, Advances in Science and Technolohy **45**, 2169 (2006).
[3] N.L. Freitas, J.P. Continho, M.C. Silva, H.L. Lira, R.H.G.A. Kiminami, A.C.F.M. Costa, Materials Science Forum **660-661**, 943 (2010).
[4] Jie-Chung Lou, Chien-Kuei Chang, Environmental Engineering Science **23**, 1024 (2006).
[5] Yunzhe Feng, Protap M. Rao, Dong Rip Kim, Xiaolin Zheng, Proceeding of the Combustion Institute **33**, 3169 (2011).
[6] J.C. Lou, Y.J. Tu, J. Air & Waste Manag. Assoc. **55**, 1809 (2005).
[7] N. Chu, X. Wang, Y. Liu, H. Jin, Q. Wu, L. Li, Z. Wang, H. Ge, J. Alloys Comp. **470**, 438 (2009).
[8] A.B. Gadkari, T.J. Shinde, P.N. Vasambekar, Mater. Chem. Phys. **114**, 505 (2009).
[9] C.V. Gopal Reddy, S.V. Manorama, V.J. Rao, Sensors and Actuators B: Chemical **55**, 90 (1999).
[10] P.A. Jadhav, R.S. Devan, Y.D. Kolekar, B.K. Chougule, J. Phy. Chem. Solids **70**, 396 (2009).
[11] S. Prasad, N.S. Gajbhiye, J. Alloys Comp. **265**, 87 (1998).
[12] S. Komarneni, E. Fregeau, E. Breval, R. Roy, J. Am. Ceram.Soc. Commun. **71**, C26 (1988).
[13] X. Li, G. Wang, J. Magn. Magn. Mater. **321**, 1276 (2009).
[14] R.V. Mangalaraja, S. Thomas Lee, S. Ananthakumar, P. Manohar, C.P. Camurri, Mater. Sci. Eng.:A **476**, 234 (2008).
[15] P.D.Popa, N.Rezlescu, Gh.Iacob, A new procedure for preparing ferrite powders, Romanian Patent No.121300, OSIM, Bucarest, 2008.
[16] N. Rezlescu, C. Doroftei, E. Rezlescu, P.D. Popa, Sensors and Actuators B: Chemical **133**, 420 (2008) .
[17] P.D.Popa and N.Rezlescu, Rom. Rep. Phys. **52**, 769 (2000).
[18] V.R. Choudhary, S. Banerjee, S.G. Pataskar, Proc. Indian Acad. Sci. (Chem.Sci) **115**, 287 (2003).
[19] P.O. Thevenin, P.G. Menon, S.G. Jaras, Cattech **7**, 10 (2003).
[20] H. Klung, L. Alexander, X-ray Diffraction Procedures, Wiley, New York, 1962.
[21] S. Lowell, J.E. Shields, M.A. Thomas, M. Thommes, Characterization of Porous Solids and Powders: Surface Area, Pore Size and Density. Kluwer Academic Publishers, Dordrecht/Boston/London, 2004.
[22] J. Smit, H.P.J. Wijn, Les Ferrites, Dunod, Paris, 1961.
[23] J.E. Huheey, E.A. Keiter, R.J. Keiter, Chemistry. Principles of structure and reactivity, Harper Collins, College Publishers, 1993.
[24] A. Machocki, T. Ioannides, B. Stasinska, W. Gac, G. Avgouropoulos, D. Delimaris, W. Grzegorczyk, S. Pasieczna, J. Catal. **227**, 282 (2004).
[25] S.Q. Li, H.T. Liu, L.A. Yan, X.L. Wang, Vatal. Commun. **8**, 237 (2007).
[26] S.Q. Li, X.L. Wang, Catal. Commun. **8**, 410 (2007).
[27] C. Li, K. Domen, K. Maruya, T. Onishi, J. Am. Chem.Soc **111**, 7683 (1989).